

Chapter 1

Theoretical and Experimental Overview

1.1 Deep Inelastic Scattering

To understand the structure of the nucleon it is useful to first introduce the original process which described the nucleon as having a sub-structure. This process is the Deep Inelastic Scattering (DIS) process where a lepton impinges on a nucleon denoted as

$$l(\ell) + N(P) \rightarrow l(\ell') + X(P_X), \quad (1.1)$$

where l denotes a lepton, N denotes a nucleon, X represents all products not detected and ℓ , ℓ' , P and P_X are the four momentum for their respective lepton or nucleon. This process is an electromagnetic reaction where a the lepton is scattered via virtual photon exchange with the nucleon. The leading order Feynman diagram for this reaction is shown in Fig. 1.1.

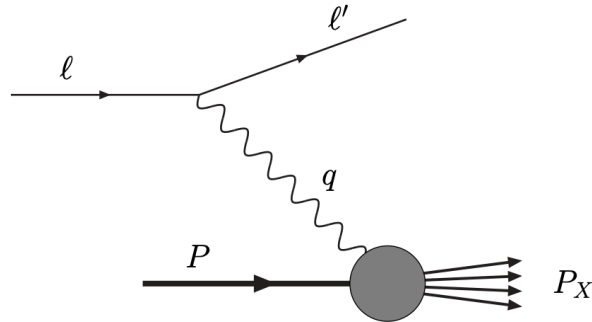


Figure 1.1: The leading order Feynman diagram for deep inelastic scattering

DIS is traditionally studied with a high energy lepton beam and a fixed nuclear target. The initial state kinematics are described by

$$s = (\ell + P)^2 \quad \text{or} \quad E, \quad (1.2)$$

where s is the center of mass energy and E is the energy of the lepton beam. The detected reaction kinematics in the lab frame are described by

$$Q^2 = -q^2 = -(\ell - \ell')^2 \approx EE'(1 - \cos \theta) \quad (1.3)$$

$$x = \frac{Q^2}{2P \cdot q} = \frac{Q^2}{2M\nu} \quad (1.4)$$

$$\nu = E - E' \quad (1.5)$$

$$y = \frac{P \cdot q}{P \cdot \ell} = \frac{E - E'}{E} = \frac{\nu}{E} \quad (1.6)$$

$$W^2 = (P + q)^2 \quad (1.7)$$

where q is the virtual photon four momentum, E' is the scattered leptons energy, x is Bjorken x , ν is the change in energy of the scattered lepton, y is the inelasticity and W^2 is invariant mass of hadron final state. In the last relation from Eq. 1.3, θ is the scattering angle of the lepton with respect to the beam and the approximation is only true when the lepton mass is assumed to be zero. In Eq. 1.4, M is the nucleon mass. In the parton model, section 1.2, x has the interpretation as being the momentum fraction of the struck parton with respect to its parent hadron and therefore x ranges between 0 and 1. The inelasticity, y , measure the proportional lepton energy reduction and therefore takes on a value between 0 and 1.

The process is called deep if $Q^2 \gg M^2$ and inelastic if $y < 1$. For practical purposes in experiments, the deep inelastic criteria corresponds to a $Q^2 > 1 \text{ GeV}$ and $W^2 > M^2$. As can be seen in Eq. [1.3-1.7], not all the variables are independent. DIS is described by two independent variables usually given by (x, Q^2) or (x, y) . For reference, in the limit as $y \rightarrow 1$ the process becomes elastic scattering and can then be described by only one independent variable.

The cross-section for DIS is defined as [5]

$$d\sigma = \frac{1}{4P \cdot \ell} \frac{e^4}{Q^4} L_{\mu\nu} W^{\mu\nu} 2\pi \frac{d^3\ell'}{(2\pi)^3 2E'} \quad (1.8)$$

where $L_{\mu\nu}$ is the leptonic tensor and $W^{\mu\nu}$ is the hadronic tensor. The leptonic tensor describes free leptons and can therefore be calculated in perturbation theory. It can be decomposed into a systematic spin-independent tensor and an anti-symmetric spin-dependent tensor. Summing over all the possible spins of the lepton beam, the leptonic tensor is

$$L_{\mu\nu} = 2\left(\ell_\mu \ell'_\nu + \ell_\nu \ell'_\mu - g_{\mu\nu} \ell \cdot \ell'\right) + 2m\epsilon_{\mu\nu\rho\sigma} s^\rho q^\sigma \quad (1.9)$$

where m is the lepton mass and s^ρ is the spin four vector of the lepton.

Generically the hadronic tensor is defined as

$$W^{\mu\nu} = \frac{1}{2\pi} \int d^4\xi e^{iq\cdot\xi} \langle PS | J^\mu(\xi) J^\nu(0) | PS \rangle \quad (1.10)$$

where J is an electromagnetic current and $|PS\rangle$ represents the nucleon with momentum P and spin S . The hadronic tensor describes a hadron bound together by quantum chromo-dynamics (QCD). As of yet there is no known technique for calculating the hadronic tensor in a perturbation theory or otherwise. Instead the hadronic tensor can be written in the most general Lorentz invariant form using structure functions to parameterize the non-perturbative nature of the tensor. With the use of these structure functions, the differential DIS cross-section can be written

$$\frac{d\sigma}{dx dy} = \frac{8\pi\alpha^2 ME}{Q^4} \left\{ xy^2 F_1(x, Q^2) + (1-y) \frac{F_2(x, Q^2)}{x} + c_1(y, \frac{Q^2}{\nu}) g_1(x, Q^2) + c_2(y, \frac{Q^2}{\nu}) g_2(x, Q^2) \right\} \quad (1.11)$$

where α is the electromagnetic coupling constant; F_1 , F_2 , g_1 , g_2 are structure functions; and c_1 and c_2 are functions which depend on the polarization of the target. The SLAC collaboration measured the structure functions, F_1 and F_2 , and found mild variations as a function Q^2 [7, 9]. This phenomenon now known as Bjorken scaling lead to the theory of the parton model [6]. Fig. 1.2 shows the F_2 structure function which is approximately constant as a function of Q^2 .

1.2 The Parton Model

The parton model is described in what is called an infinite momentum frame where the nucleon is moving which large momentum. In the parton model the nucleon, in high energy scattering processes, is considered to be composed of point like constituent mass-less particles called partons. At high energy scattering the QCD strong force binding the partons becomes asymptotic small and therefore the partons appear to be free. The cross-section in DIS can then be described as a lepton scattering incoherently off a free parton in the nucleon. In the parton model the hadron tensor for scattering off a quark can be written as [5]

$$W^{\mu\nu} = \frac{1}{2\pi} \sum_q e_q^2 \sum_X \int \frac{d^3 P_X}{(2\pi)^3 2E_X} \int \frac{d^4 k}{(2\pi)^4} \int \frac{d^4 k'}{(2\pi)^4} \delta(k'^2) \quad (1.12)$$

$$\times [\bar{u}(k') \gamma^\mu \langle X | u(k) | PS \rangle] * [\bar{u}(k') \gamma^\nu \langle X | u(k) | PS \rangle] \times (2\pi)^4 \delta^4(P - k - P_X) (2\pi)^4 \delta^4(k + q - k'),$$

where e_q is the electric charge of quark flavor q ; and u and \bar{u} are free Dirac spinors. This hadronic tensor can be simplified by introducing the quark-quark correlation matrix as

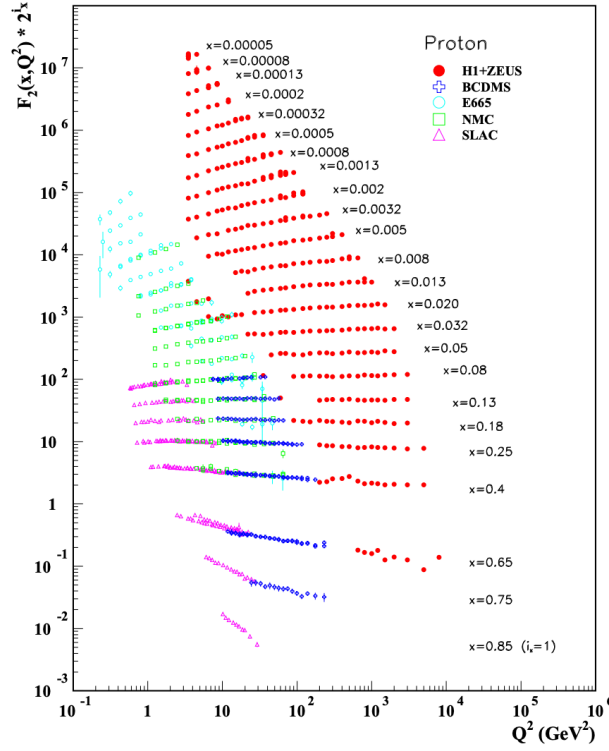


Figure 1.2: The F_2 structure function measured by several experiments. Note that the data is shifted up by a factor 2^{i_x} to see the x dependence. Image taken from [21]

$$\Theta_{ij}(k, P, S) = \sum_X \int \frac{d^3 P_X}{(2\pi)^3 2E_X} (2\pi)^4 \delta^4(P - k - P_X) \times \langle PS | \phi_j(0) | X \rangle \langle X | \phi_i(0) | PS \rangle, \quad (1.13)$$

where $\phi(\xi) = e^{-ip \cdot \xi} u(p)$ is a quark field. Using the quark-quark correlation matrix, the hadronic tensor can be written as

$$W^{\mu\nu} = \sum_q e_q^2 \int \frac{d^4 k}{(2\pi)^4} \int \frac{d^4 k'}{(2\pi)^4} \delta(k'^2) (2\pi)^4 \delta^4(k + q - k') \times \text{Tr}[\Theta \gamma^\mu \not{k}' \gamma^\nu]. \quad (1.14)$$

In the cases of unpolarized or longitudinally polarized DIS the lead order contributing terms from the quark-quark correlator are [4, 8, 16]

$$\Theta = \frac{1}{2} \left(f_1(x) \not{P} + g_{1L}(x) \lambda \gamma_5 \not{P} \right) \quad (1.15)$$

where λ is the longitudinal polarization of the hadron. The hadronic tensor simplifies to a symmetric contribution and an anti-symmetric contribution [5]

$$W_{\mu\nu}^{\text{symmetric}} = \frac{1}{P \cdot q} \sum_q e_q^2 \left((k_\mu + q_\mu) P_\nu + (k_\nu + q_\nu) P_\mu - g_{\mu\nu} \right) f_1^q(x), \quad (1.16)$$

$$W_{\mu\nu}^{\text{anti-symmetric}} = \lambda \epsilon_{\mu\nu\rho\sigma} (k_\nu + q_\nu) P^\rho \sum_q e_q^2 g_{1L}^q(x), \quad (1.17)$$

where in Eq. 1.15 f_1 and g_1 are two parton distribution functions (PDFs). f_1 is interpreted as the quark number density and g_{1L} is interpreted as the total quark helicity distribution in a hadron. f_1 then refers to the density of unpolarized quarks in a hadron and g_{1L} refers to the density of quarks longitudinally polarized in the same longitudinal direction as the hadron. To make this explicit, f_1 and g_{1L} can be written

$$f_1 = f_1^+ + f_1^-, \quad (1.18) \quad g_{1L} = f_1^+ - f_1^-, \quad (1.19)$$

where $+$ and $-$ denote the helicity. To be clear the parton distribution g_{1L} is not the same as the structure function g_1 .

The unpolarized quark number density, f_1 , has been extracted from global analysis of several experiments [18]. Fig. 1.3 shows the current xf_1 values and confidence intervals for different quarks and gluons specifically in the proton.

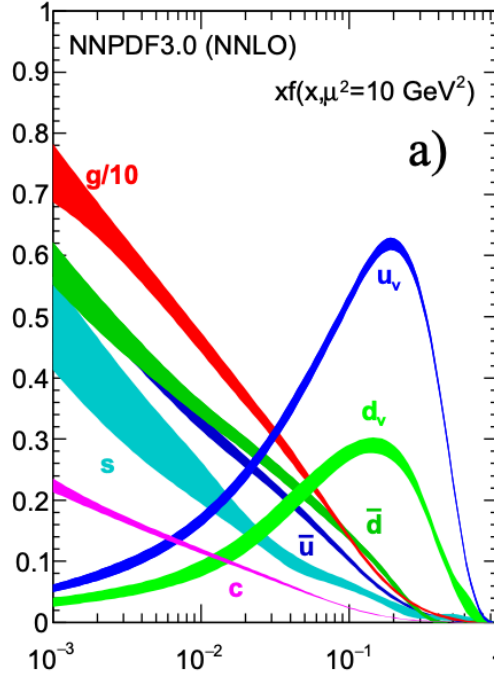


Figure 1.3: The unpolarized parton distribution functions times the momentum fraction. The different color correspond to different quarks or gluons. Image taken from [21]

The longitudinal spin structure, g_{1L} has also been measured at SMC, HERMES, and COMPASS [2, 3,

19]. The global analysis fit is shown in Fig. 1.4 using the parameterizations from NNPDF2014, AAC2008, DSSV2008 and LSS2010 [1, 14, 15, 17].

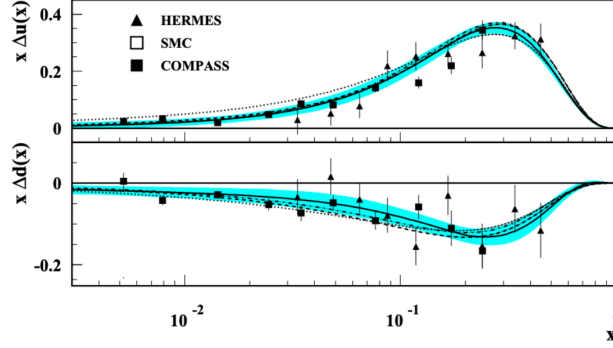


Figure 1.4: The longitudinally polarized parton distribution functions times the momentum fraction for the u-quark (top) and the d-quark (bottom). Image taken from [21]

In the parton model the structure function F_1 and F_2 are related to each other and to the unpolarized quark number as

$$F_2(x) = 2xF_1(x) = \sum_q e_q^2 x (f_1^q + f_1^{\bar{q}}) \quad (1.20)$$

which is known as the Callan-Gross relation [12]. As well the structure function g_1 is related to the helicity distribution, g_{1L} , as

$$g_1(x) = \frac{1}{2} \sum_q e_q^2 g_{1L}(x). \quad (1.21)$$

1.3 Transverse Momentum Dependence

The transverse momentum of the partons is integrated over when measuring the DIS process. This is because only the scattered lepton is measured and any transverse parton motion cannot be measured. The Drell-Yan process 1.4 and the SIDIS process 1.5 however are sensitive to the internal transverse momentum of the partons. When including the transverse parton momentum, the most generic leading order quark-quark correlator can be written [4, 8, 16]

$$\begin{aligned} \Theta = & \frac{1}{2} \left[f_1(x, k_\perp) \not{P} + \frac{1}{M} h_1^\perp(x, k_\perp) \sigma^{\mu\nu} k_\mu P_\nu + g_{1L}(x, k_\perp) \lambda \gamma_5 \not{P} \right. \\ & + \frac{1}{M} g_{1T}(x, k_\perp) \gamma_5 \not{P} (k_\perp \cdot S_\perp) + \frac{1}{M} h_{1L}(x, k_\perp) \lambda i \sigma_{\mu\nu} \gamma_5 P^\mu k_\perp^\nu + h_1(x, k_\perp) i \sigma_{\mu\nu} \gamma_5 P^\mu S_\perp^\nu \\ & \left. + \frac{1}{M^2} h_{1T}^\perp(x, k_\perp) i \sigma_{\mu\nu} \gamma_5 P^\mu \left(k_\perp \cdot S_\perp k_\perp^\nu - \frac{1}{2} k_\perp^2 S_\perp^\nu \right) + \frac{1}{M} f_{1T}^\perp(x, k_\perp) \epsilon^{\mu\nu\rho\sigma} \gamma_\mu P_\nu k_\rho S_\sigma \right], \end{aligned} \quad (1.22)$$

where k_\perp denotes the transverse parton momentum and S_\perp denotes the transverse hadron spin. Eq. 1.22 includes eight transverse momentum dependent (TMD) PDFs which are functions of x and k_\perp . The notation

used to depict the TMDs functions is the so-called Amsterdam notation. The letters represent the different quark polarizations where f, g, h stand for unpolarized, longitudinally polarized and transversely polarized respectively. The subscript 1 denotes leading order and the subscripts T and L denote a transversely polarized hadron and a longitudinally polarized hadron respectively. Finally the superscript \perp denotes that the distribution is an odd function of k_{\perp} and therefore is zero when integrated over the parton transverse momentum. Fig. 1.5 organizes the TMDs by nucleon and quark polarizations and gives a visual of each TMD's interpretation.


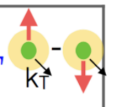

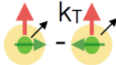



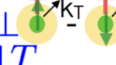
		Nucleon		
		Unpolarized	Longitudinal	Transverse
Quark	Unpolarized	f_1  number density		f_{1T}^{\perp}  Sivers
	Longitudinal		g_{1L}  helicity	g_{1T}  worm-gear T
	Transverse	h_1^{\perp}  Boer-Mulders	h_{1L}^{\perp}  worm-gear L	h_1  transversity h_{1T}^{\perp}  pretzelosity

Figure 1.5: The eight TMDs needed to describe a spin 1/2 nucleon at leading order. The columns represent the different nucleon polarization and the rows represent the different quark polarizations. The individual figures give a visual of the TMD's interpretation.

1.3.1 Sivers Distribution

The Sivers TMD was first purposed to explain large nucleon spin-dependent asymmetries [20]. The interpretation of the Sivers TMD, $f_{1T}^{q\perp}(x, \mathbf{k}_T)$, is that it gives a correlation between transverse spin of the parent hadron and transverse momentum of parton. When viewing the hadron in the direction of it's momentum, if $f_{1T}^{q\perp}(x, \mathbf{k}_T)$ is positive then it is expected that there are more partons with momentum going left than going right. Intuitively a non-zero $f_{1T}^{q\perp}(x, \mathbf{k}_T)$ would then imply that the bound quarks carry orbital angular momentum. As of yet however, there is no theoretical link between orbital angular momentum and the Sivers function.

The Sivers function is odd under time reversal. As a result of this it was originally believe to be a forbidden correlation. However it was shown that the Sivers function could be non-zero from gluon exchange

during the initial state in the Drell-Yan process and during the final state in SIDIS [10, 11]. Surprising it was shown that a non-zero Sivers function is expected to have opposite sign in SIDIS and Drell-Yan [13]. That is

$$f_{1T}^\perp|_{Drell-Yan} = -f_{1T}^\perp|_{SIDIS}. \quad (1.23)$$

give sivers SIDIS results from HERMES/COMPASS. Give interpretation

1.4 Drell-Yan

1.5 Semi-Inclusive Deep Inelastic Scattering

$$\begin{aligned} W_{\mu\nu} = & \left(\frac{q_\mu q_\nu}{q^2} - g_{\mu\nu} \right) \frac{F_1(x, Q^2)}{M} + \left(P_\mu - \frac{P \cdot q}{q^2} q_\mu \right) \left(P_\nu - \frac{P \cdot q}{q^2} q_\nu \right) \frac{F_2(x, Q^2)}{M^2 \nu} \\ & + i \epsilon_{\mu\nu\rho\sigma} \frac{q^\rho}{P \cdot q} \left\{ S^\sigma g_1(x, Q^2) + \left(S^\sigma - \frac{S \cdot q}{P \cdot q} P^\sigma \right) g_2(x, Q^2) \right\}, \end{aligned} \quad (1.24)$$

where F_1 , F_2 , g_1 and g_2 are structure functions which are determined from experiments.

References

- [1] I. Abt, A. M. Cooper-Sarkar, B. Foster, V. Myronenko, K. Wichmann, and M. Wing. Study of HERA ep data at low Q^2 and low x_{Bj} and the need for higher-twist corrections to standard perturbative QCD fits. *Phys. Rev.*, D94(3):034032, 2016.
- [2] B. Adeva et al. The Spin dependent structure function $g(1)$ (x) of the proton from polarized deep inelastic muon scattering. *Phys. Lett.*, B412:414–424, 1997.
- [3] A. et al. Airapetian. Flavor decomposition of the sea-quark helicity distributions in the nucleon from semiinclusive deep inelastic scattering. *Phys. Rev. Lett.*, 92:012005, Jan 2004.
- [4] Alessandro Bacchetta, Markus Diehl, Klaus Goeke, Andreas Metz, Piet J. Mulders, and Marc Schlegel. Semi-inclusive deep inelastic scattering at small transverse momentum. *JHEP*, 02:093, 2007.
- [5] Vincenzo Barone, Alessandro Drago, and Philip G. Ratcliffe. Transverse polarisation of quarks in hadrons. *Phys. Rept.*, 359:1–168, 2002.
- [6] J. D. Bjorken and Emmanuel A. Paschos. Inelastic Electron Proton and gamma Proton Scattering, and the Structure of the Nucleon. *Phys. Rev.*, 185:1975–1982, 1969.
- [7] Elliott D. Bloom et al. High-Energy Inelastic e p Scattering at 6-Degrees and 10-Degrees. *Phys. Rev. Lett.*, 23:930–934, 1969.
- [8] Daniel Boer and P. J. Mulders. Time reversal odd distribution functions in leptonproduction. *Phys. Rev.*, D57:5780–5786, 1998.
- [9] Martin Breidenbach, Jerome I. Friedman, Henry W. Kendall, Elliott D. Bloom, D. H. Coward, H. C. DeStaebler, J. Drees, Luke W. Mo, and Richard E. Taylor. Observed Behavior of Highly Inelastic electron-Proton Scattering. *Phys. Rev. Lett.*, 23:935–939, 1969.
- [10] Stanley J. Brodsky, Dae Sung Hwang, and Ivan Schmidt. Final state interactions and single spin asymmetries in semiinclusive deep inelastic scattering. *Phys. Lett.*, B530:99–107, 2002.
- [11] Stanley J. Brodsky, Dae Sung Hwang, and Ivan Schmidt. Initial state interactions and single spin asymmetries in Drell-Yan processes. *Nucl. Phys.*, B642:344–356, 2002.
- [12] C. G. Callan and David J. Gross. High-energy electroproduction and the constitution of the electric current. *Phys. Rev. Lett.*, 22:156–159, Jan 1969.
- [13] John C. Collins. Leading twist single transverse-spin asymmetries: Drell-Yan and deep inelastic scattering. *Phys. Lett.*, B536:43–48, 2002.
- [14] L. A. Harland-Lang, A. D. Martin, P. Motylinski, and R. S. Thorne. The impact of the final HERA combined data on PDFs obtained from a global fit. *Eur. Phys. J.*, C76(4):186, 2016.
- [15] M. Hirai and S. Kumano. Determination of gluon polarization from deep inelastic scattering and collider data. *Nucl. Phys.*, B813:106–122, 2009.

- [16] P. J. Mulders and R. D. Tangerman. The Complete tree level result up to order $1/Q$ for polarized deep inelastic leptonproduction. *Nucl. Phys.*, B461:197–237, 1996. [Erratum: *Nucl. Phys.*B484,538(1997)].
- [17] Emanuele R. Nocera, Richard D. Ball, Stefano Forte, Giovanni Ridolfi, and Juan Rojo. A first unbiased global determination of polarized PDFs and their uncertainties. *Nucl. Phys.*, B887:276–308, 2014.
- [18] Juan Rojo, Alberto Accardi, Richard D Ball, Amanda Cooper-Sarkar, Albert de Roeck, Stephen Farry, James Ferrando, Stefano Forte, Jun Gao, Lucian Harland-Lang, Joey Huston, Alexander Glazov, Maxime Gouzevitch, Claire Gwenlan, Katerina Lipka, Mykhailo Lisovyi, Michelangelo Mangano, Pavel Nadolsky, Luca Perrozzi, Ringaile Plačakytė, Voica Radescu, Gavin P Salam, and Robert Thorne. The PDF4lhc report on PDFs and LHC data: results from run i and preparation for run II. *Journal of Physics G: Nuclear and Particle Physics*, 42(10):103103, sep 2015.
- [19] I. A. Savin. COMPASS results on the nucleon spin structure. *Nucl. Phys. Proc. Suppl.*, 219-220:94–101, 2011.
- [20] Dennis W. Sivers. Single Spin Production Asymmetries from the Hard Scattering of Point-Like Constituents. *Phys. Rev.*, D41:83, 1990.
- [21] M. Tanabashi et al. Review of Particle Physics. *Phys. Rev.*, D98(3):030001, 2018.